

Battery-Free Wireless Node Powered using High-Efficiency Harvesting of 900 MHz GFSK-Modulated Packets with a Compact Rectenna

Mahmoud Wagih, *Member, IEEE*

School of Electronics and Computer Science, University of Southampton, Southampton, United Kingdom

Mahmoud.Wagih@IEEE.org

Abstract—Radio Frequency (RF) Simultaneous Wireless Information and Power Transfer (SWIPT) has attracted significant interest with a range of SWIPT-specific rectenna implementations. However, the impact of modulated waveforms on a capacitor charging time remains unknown, and a system powered off packets has yet to be demonstrated. This paper presents an RF-powered sub-1 GHz sensor node through modulated packages with a sub-0 dBm sensitivity without any DC-DC power management circuitry. Using Gaussian Frequency Shift Keying (GFSK) modulated signals from a commercial IoT transceiver, the RF-DC power conversion efficiency (PCE) is investigated for both a resistive and capacitive load. It is shown that GFSK modulation with varying data rates has minimal influence on the PCE. A miniaturized rectenna is demonstrated charging a supercapacitor powering a sub-1 GHz sensor node for over 32 s, charged using 40 GFSK packets transmitted in 62 s, at 1.6 m from a 4 W circularly-polarized source at 900 MHz. The demonstrated rectenna exhibits over an order of magnitude improvement in the sensitivity over previous works harvesting modulated packets.

Index Terms—Gaussian Frequency Shift Keying (GFSK), modulation, rectifier, rectenna, Simultaneous Wireless Information and Power Transfer (SWIPT), supercapacitor, wireless power transmission (WPT)

I. INTRODUCTION

As the energy demands of Internet of Things (IoT) networks continue to increase, Wireless Power Transmission (WPT) is increasingly seen as an alternative to batteries which has already been demonstrated in millions of Radio Frequency Identification (RFID) tags [1]. Simultaneous Wireless Information and Power Transfer (SWIPT) is increasingly cited as the future of power-autonomous wireless networks, with an array of network architectures proposed for SWIPT [2].

Beyond theoretical networking studies [2], the practical implementation of SWIPT can be divided into a rectenna and rectifier design problem, and a signal and waveform design problem. Multiple rectennas including dual-band microstrip SWIPT rectennas [3], single-band dual-polarized RFID tags [4], and full-duplex multi-in multi-out (MIMO) [5] SWIPT antennas/rectennas have been proposed based on shared aperture multi-port antennas which do not need a matching network. Furthermore, hybrid couplers have been proposed

This work was supported by the Royal Academy of Engineering and the Office of the Chief Science Adviser for National Security under the UK Intelligence Community Postdoctoral Research Fellowship programme.

for optimal power-splitting for rectennas involving the use of 50 Ω -matched antennas and rectifiers [6]. While the aforementioned rectennas achieved a state-of-the-art RF-to-DC Power Conversion Efficiency (PCE) based on high-sensitivity well-matched rectifiers, they were mostly characterized under Continuous Wave (CW) excitation.

On the signal and wave-form design end, several research efforts have dealt with wave-form design for optimal PCE including multi-sine waveforms [7], as well as variable Peak-to-Average Power Ratios (PAPRs) [8], [9]. In addition, the impact of modulated signals on the rectifier's PCE has been investigated alongside a co-optimized rectifier design [10]. However, these efforts have focused on waveform design to improve the rectifier's PCE as opposed to using *existing* modulated signals, used in IoT communication, for SWIPT.

On the other hand, a sub-1 GHz IoT transceiver was used to demonstrate the feasibility of RF WPT using packets based on an off-the-shelf Powercast rectifier [11]. However, the PCE was roughly under 5%, significantly lower than conventional rectifiers at power levels between 0 and 15 dBm. Furthermore, while RF energy harvesting from Gaussian Frequency Shift Keying (GFSK)-modulated Bluetooth Low Energy (BLE) packets was demonstrated with a 20 cm wireless range, using a high-efficiency rectifier, such approach is limited by the low transmitted power level of BLE, and hence was not used to power a system, and could only yield a nJ-level energy [12].

In this paper, a Wireless Sensor Node (WSN) powered using GFSK sub-1 GHz IoT signals is presented, achieving at least 8 \times longer range than previous works powered from packets, and over 10 dB higher sensitivity and efficiency than reported off-the-shelf RF power harvesters collecting packets. The demonstration of a WSN based on off-the-shelf components, for the first time, being powered using packets proves the concept of far-field SWIPT.

II. WSN AND RFEH SYSTEM DESIGN

Sub-1 GHz WSNs have the advantage of a long range of operation at a relatively low power consumption [13]. In the context of SWIPT, the WPT is often implemented in the lower frequency band. In several recent SWIPT implementations, the sub-1 GHz license-free band is often used for WPT where the 2.4 GHz or the 3–10 GHz spectrum is used for communication [3], [14]. Therefore, this work focuses on

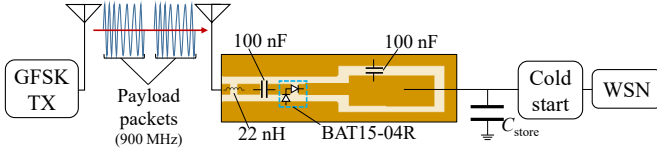


Fig. 1. The proposed system for packet-based WPT using GFSK modulated IoT signals.

harvesting the signals from a conventional sub-1 GHz IoT transceiver, acting as a gateway, to power edge nodes. The gateway and edge nodes are based on Texas Instruments Sub-1 GHz CC1130 transceiver “Launchpad” development boards.

The rectifier investigated is a coplanar waveguide (CPW) voltage doubler implemented on a flexible substrate. The diode used is the BAT15-04R, owing to its 4 V breakdown voltage, which can generate up to 8 V DC output in a voltage doubler configuration. The rectifier is matched for a 900 MHz input with a low optimum load impedance, optimized using harmonic balance simulation in ADS. The output of the rectifier is directly connected to an energy storage capacitor (in the mF range) to power the WSN periodically once the turn-on threshold voltage is reached. The rectifier is shown in Fig. 1, with the exact dimensions based on [15].

III. RECTIFIER AND SYSTEM CHARACTERIZATION

A. CW vs. Modulated Rectifier Response

First of all, the DC output of the rectifier is characterized using a CW input from a VNA’s signal generator. Fig. 2 shows the harmonic balance simulated (using Keysight ADS) and measured output of the rectifier at 900 MHz, in close agreement. The large-signal diode model of the BAT15-04R has been modified to have a saturation current $I_S=1\times10^{-8}$, which mitigates the discrepancy previously observed in [15], when the same diode model was used in a voltage doubler rectifier. A resistive load of $3\text{ k}\Omega$ was chosen following an experimental and HB-simulated load sweep at 0 dBm.

The CC1130 transmitter is then programmed to act as a CW unmodulated source and its power output is measured using a power meter. As the CC1130, with an on-board PA can only generate a signal at discrete power points between 7 and 26 dBm, a -3 dB and -20 dB attenuator were connected to its output to realize a sub-0 dBm input, which would be more representative of real-world far-field WPT scenarios. The CC1130 was then set to transmit continuously as a modulated source at two data rates, 50 KBPS and 200 KBPS, with the output fed into the rectifier, after the power level was verified using the VNA’s receiver. The rectifier’s DC output for the modulated excitation is shown alongside the CW response in Fig. 2, where it can be seen that the PCE closely matches that of the CW input. While a larger discrepancy is noticeable in Fig. 1(a), the voltage output in Fig. 1(b) shows minimal variations which could be attributed to measurement errors in the oscilloscope/probe. The slightly increased PCE for a higher data-rate could be attributed to the wider bandwidth of the signal resulting in more tones at the rectifier’s input

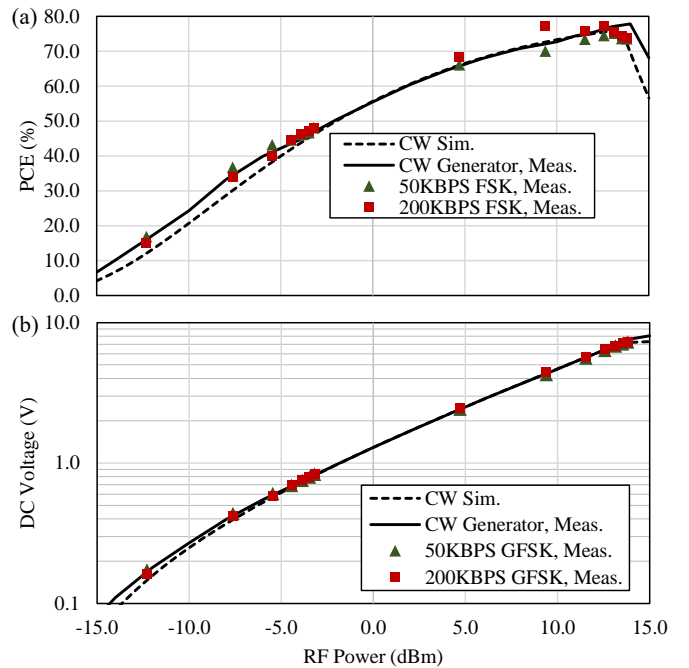


Fig. 2. Simulated and measured PCE (a) and DC voltage output across the optimal $3\text{ k}\Omega$ load (b) for CW and GFSK signals of different data-rates.

B. Energy Harvesting and Storage from packets

Having verified that GFSK modulation with varying bit-rates has a minimal influence on the rectifier’s output, the next step is exploring the impact of packet length and data-rate on the PCE and net energy yield. The optimal resistive load was replaced with a capacitive load, i.e. an energy storage device, which can then be used to power a WSN.

Firstly, a 1 mF electrolytic capacitor is used in conjunction with the rectifier. Instead of a continuous modulated transmission, which was shown to have minimal influence on the PCE, modulated packets of a finite length are used. The transmitter is programmed to transmit a 255 8 bit-long characters payload at a measured power output of 4.7 dBm (after the 3 dB attenuator and coaxial adapters). The transceiver’s 4.7 dBm output is fed to the capacitor-loaded rectifier. A 200 ms downtime between packets is programmed to maintain compliance with the EU EN 302 208 standard for radiated power for UHF RFID readers, requiring at least 100 m downtime for active transmissions up to 4 s.

Fig. 3 shows the measured DC voltage across the capacitor while the packets are being transmitted and harvested by the rectifier, using a 1.2 and 50 KBPS data-rate for the same pay-load. The higher data-rate will result in a much shorter packet transmission time leading to a very low DC power output from the rectifier. This in turn leads to the capacitor being charged for very short periods, shown in the shaded regions in Fig. 3(b). On the other hand, when the same payload is transmitted using a low data-rate, each active charging period is over $20\times$ longer, leading to more efficient capacitor charging, as in Fig. 3. The average charging efficiency for the

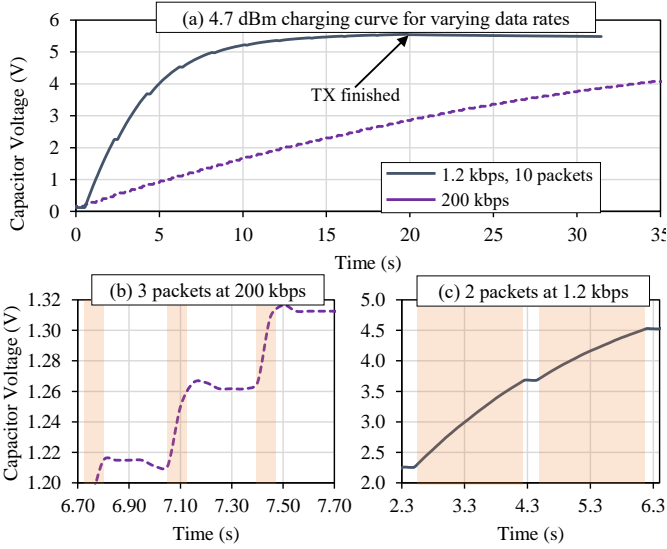


Fig. 3. Measured V_C of the 1 mF electrolytic capacitor while being charged from packets of varying data-rates for a 4.7 dBm input: (a) full charging curve; (b) 3 packets at 200 kbps; (c) 2 packets at 1.2 kbps; shaded regions indicate active packet transmission.

first four seconds in Fig. 3 is calculated using

$$PCE_{\text{average}} = \frac{CV^2}{2} \times \frac{1}{P_{\text{RF}}} \times \frac{1}{t} \quad (1)$$

for $t=4.2$ (i.e. the first 4.2 s of operation), $P_{\text{RF}}=4.7$ dBm, and $C=1$ mF. For the 200 KBPS and 1.2 KBPS transmission data-rates, PCE_{average} are 54% and 2.6%, respectively, demonstrating the benefits of a low data-rate for WPT.

The observed response shows that when the GFSK modulated signal is being transmitted the capacitor could be charged continuously with a similar response to a CW charging curve [15], which is attributed to the similar PCE for a CW and GFSK excitation, previously shown in Fig. 2. Furthermore, this is in line with previous works which have harvested Frequency Modulated (FM) signals from handheld two-way radios in the near-field, sufficing a DC-DC power management circuit [16] and charging a supercapacitor [17].

C. Wireless Testing and WSN Powering

In order to demonstrate the complete packet-based WPT system, the CC1310-based transmitter is connected to a low-cost in-house RF PA matched around 900 MHz. The power output from the PA was measured to be around 29 dBm (approximately 1 W). The output of the PA is fed into a circularly-polarized broadside antenna with 8 dBi gain. Considering the insertion losses in the adapters and the coaxial cable between the patch and the PA, an equivalent isotropic radiated power (EIRP) of 36 dBm is expected. The rectenna is positioned at 1.6 m away from the source and its output is connected directly to the 22 mF supercapacitor, with the capacitor voltage and current consumption of the load WSN monitored using an oscilloscope. Fig. 4 shows a photograph of the measurement setup of the rectenna.

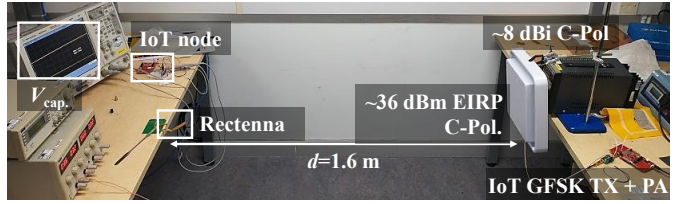


Fig. 4. Photograph of the wireless measurement setup of the rectenna with a GFSK-modulated circularly-polarized 36 dBm EIRP source.

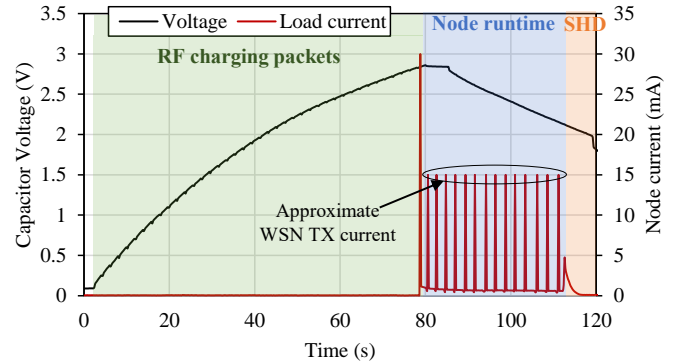


Fig. 5. Measured wireless charging voltage curve of the 22 mF capacitor, from $S=17.3 \mu\text{W}/\text{cm}^2$, and the WSN approximate current consumption.

As a circularly-polarized source is used, to minimize the impact of polarization misalignment at the receiver [18], [19], up to 50% of the incident plane wave can be received by the linearly-polarized monopole. The incident power density S at the rectenna is given by

$$S = \frac{P_{\text{TX}}G_{\text{TX}}}{4\pi d^2} \quad (2)$$

and is calculated to be $17.28 \mu\text{W}/\text{cm}^2$ based on a 33 dBm copolarized EIRP. Assuming a 2 dBi receiver gain based on the meandered monopole [15], the received power by the rectifier is estimated to be -0.61 dBm, using the free-space path loss model.

Fig. 5 shows the charging curve of the 22 mF supercapacitor up to 2.8 V, translating to approximately 86 mJ of energy. This energy level is reached after receiving 40 packets. The capacitor then discharges into the WSN which is programmed to transmit approximately every 100 ms for ten packets (4-byte payload), before dropping to a 1 s transmission period. The current consumption trace in Fig. 5 shows the approximate response of the WSN, limited by the quantization of the oscilloscope missing some of the transmission peaks, which last for under 5 ms each. Once the capacitor voltage drops below 2.2 V the WSN shuts down and can then be recharged wirelessly again. Based on this successful demonstration of a packet-powered WSN, far-field SWIPT using off-the-shelf components represents a feasible proposition. The range of operation and sub-0 dBm sensitivity can be significantly improved by using a state-of-the-art multi-stage voltage multiplying CMOS rectifier [14], as well as low-voltage WSNs.

TABLE I
COMPARISON WITH OTHER MODULATED “PACKET” HARVESTERS

	This work	[11]	[12]
Frequency	900 MHz	915 MHz	2,426 MHz
Modulation	GFSK (IoT transceiver)	IoT transceiver	BLE GFSK
Rectifier	Flexible CPW voltage doubler	Powercast P2110	Microstrip single-series
Wireless range	1.6 m	N/A	20 cm
Incident S	17.3 $\mu\text{W}/\text{cm}^2$	N/A, 9 dBm source	0.5 $\mu\text{W}/\text{cm}^2$
Modulated PCE @ 10 dBm	77% (resistive load); 53% (capacitor charging)	<5% (resistive load)	60% (resistive load)
Energy per packet	2.15 mJ @ 17.3 $\mu\text{W}/\text{cm}^2$	12.5 nJ (@9 dBm)	1.3 nJ @ 0.5 $\mu\text{W}/\text{cm}^2$
Load powered	Supercapacitor + WSN	Capacitor	Resistor

Recent works reporting RF energy harvesting from packets are compared in Table I. Compared to an off-the-shelf rectifier operating at the same frequency and using a modulated source based on the same transceiver, it can be seen that this work exhibits around 10 dB improvement in the sensitivity, by operating below 0 dBm, highlighting the significance of optimal rectifier design for low-impedance loading. Moreover, the orders of magnitude improvement in the energy per packet compared to [11] is attributed to the longer and lower data-rate packets used in this work, as well as the generally more efficient rectifier. On the other hand, the previous work at 2.4 GHz was aimed at BLE transmission which is inherently limited in the maximum transmitted power level [12]. Therefore, the $>8\times$ improvement in the operation range over [12] demonstrates the benefit of using a sub-1 GHz transmitter, where a 4 W EIRP is permitted and a low receiving antenna area loss can be maintained. Finally, to the best of our knowledge, this work is the first to demonstrate a system, based on off-the-shelf semiconductors, which can be powered from packets, starting the WSN from 40 transmitted packets roughly 2.15 mJ of harvested DC power per packet.

IV. CONCLUSION

In this paper, a wireless sensor node is demonstrated being powered through modulated RF packets with a sub-0 dBm sensitivity. Exhibiting a measured range of operation over 1.6 m and a high average PCE using a state-of-the-art high-efficiency rectifier, the proposed packet-powered sub-1 GHz rectenna represents an order of magnitude improvement in sensitivity over previous work harvesting packets in the same band, and approximately $8\times$ longer range than a Bluetooth-based system. It is concluded that using a sufficiently low data-rate and large payloads, energy can be transmitted and harvested efficiently, matching CW sources, using off-the-shelf IoT transceivers. Future work includes a power-splitting frontend with optimal power division ratio for WPT as well as demonstrating in-band communication alongside the WPT to the node.

REFERENCES

- [1] C. R. Valenta and G. D. Durgin, “Harvesting Wireless Power: Survey of Energy-Harvester Conversion Efficiency in Far-Field, Wireless Power Transfer Systems,” *IEEE Microw. Mag.*, vol. 15, 4, pp. 108–120, 2014.
- [2] T. D. P. Perera, D. N. K. Jayakody, S. K. Sharma, S. Chatzinotas, and J. Li, “Simultaneous Wireless Information and Power Transfer (SWIPT): Recent Advances and Future Challenges,” *IEEE Communication Surveys and Tutorials*, vol. 20, 1, pp. 264 – 302, 2018.
- [3] M. Wagih, G. S. Hilton, A. S. Weddell, and S. Beeby, “Dual-Band Dual-Mode Textile Antenna/Rectenna for Simultaneous Wireless Information and Power Transfer (SWIPT),” *IEEE Trans. Antennas Propag.*, 2021.
- [4] A. E. Abdulhadi and R. Abhari, “Multiport uhf rfid-tag antenna for enhanced energy harvesting of self-powered wireless sensors,” *IEEE Transactions on Industrial Informatics*, vol. 12, no. 2, pp. 801–808, 2016.
- [5] M. Wagih, G. S. Hilton, A. S. Weddell, and S. Beeby, “Dual-polarized wearable antenna/rectenna for full-duplex and mimo simultaneous wireless information and power transfer (swipt),” *IEEE Open Journal of Antennas and Propagation*, vol. 2, pp. 844–857, 2021.
- [6] P. Lu, C. Song, and K. M. Huang, “A Two-Port Multi-Polarization Rectenna with Orthogonal Hybrid Coupler for Simultaneous Wireless Information and Power Transfer (SWIPT),” *IEEE Trans. Antennas Propag.*, vol. 68 no. 10, pp. 6893 – 6905, 2020.
- [7] A. J. Soares Boaventura, A. Collado, A. Georgiadis, and N. Borges Carvalho, “Spatial power combining of multi-sine signals for wireless power transmission applications,” *IEEE Transactions on Microwave Theory and Techniques*, vol. 62, no. 4, pp. 1022–1030, 2014.
- [8] C. R. Valenta and G. D. Durgin, “Rectenna performance under power-optimized waveform excitation,” in *2013 IEEE International Conference on RFID (RFID)*, 2013.
- [9] M. H. Ouda, P. Mitcheson, and B. Clerckx, “Robust wireless power receiver for multi-tone waveforms,” in *2019 49th European Microwave Conference (EuMC)*, 2019, pp. 101–104.
- [10] F. Bolos, J. Blanco, A. Collado, and A. Georgiadis, “RF Energy Harvesting From Multi-Tone and Digitally Modulated Signals,” *IEEE Trans. Microw. Theory Techn.*, vol. 64, no. 6, pp. 1918 – 1927, 2016.
- [11] K. Lee and J. Ko, “Rf-based energy transfer through packets: Still a dream? or a dream come true?” *IEEE Access*, vol. 7, pp. 163 840–163 850, 2019.
- [12] G. Paolini, Y. Murillo, S. Claessens, D. Masotti, S. Pollin, A. Costanzo, and D. Schreurs, “Rf energy harvesting from gfsk-modulated ble signals,” in *2021 IEEE Topical Conference on Wireless Sensors and Sensor Networks (WiSNeT)*, 2021, pp. 27–29.
- [13] M. Park, “Ieee 802.11ah: sub-1-ghz license-exempt operation for the internet of things,” *IEEE Communications Magazine*, vol. 53, no. 9, pp. 145–151, 2015.
- [14] H. Lyu, Z. Wang, and A. Babakhani, “A uhf/uwb hybrid rfid tag with a 51-m energy-harvesting sensitivity for remote vital-sign monitoring,” *IEEE Transactions on Microwave Theory and Techniques*, vol. 68, no. 11, pp. 4886–4895, 2020.
- [15] M. Wagih, N. Hillier, S. Yong, A. S. Weddell, and S. Beeby, “Rf-powered wearable energy harvesting and storage module based on e-textile coplanar waveguide rectenna and supercapacitor,” *IEEE Open Journal of Antennas and Propagation*, vol. 2, pp. 302 – 314, 2021.
- [16] J. Bito, J. G. Hester, and M. M. Tentzeris, “Ambient RF Energy Harvesting From a Two-Way Talk Radio for Flexible Wearable Wireless Sensor Devices Utilizing Inkjet Printing Technologies,” *IEEE Trans. Microw. Theory Techn.*, vol. 63, 12, pp. 4533–4543, 2015.
- [17] M. Wagih, A. S. Weddell, and S. Beeby, “Dispenser printed flexible rectenna for dual-ism band high-efficiency supercapacitor charging,” in *2021 IEEE Wireless Power Transfer Conference (WPTC)*, 2021, pp. 1–4.
- [18] S. Ladan, A. B. Guntupalli, and K. Wu, “A High-Efficiency 24 GHz Rectenna Development Towards Millimeter-Wave Energy Harvesting and Wireless Power Transmission,” *IEEE Trans. Circuits And Systems*, vol. 61, 12, pp. 3358 – 3366, 2014.
- [19] M. Wagih, A. S. Weddell, and S. Beeby, “Rectennas for RF Energy Harvesting and Wireless Power Transfer: a Review of Antenna Design [Antenna Applications Corner],” *IEEE Antennas Propag. Mag.*, vol. 62 no. 5, pp. 95 – 107, 2020.